I. Measuring Vacuum Chamber Pressures with a Multifunction Data Acquisition Module

AND

II. Developing a New Technique for the Charge Calibration of Highly Segmented Silicon Arrays

C500 Report

Prepared by: James H. Black
Advisor: Dr. Romualdo T. de Souza

4 May 2006

Table of Contents

Introduction

In the following report, I describe two main projects worked on over the last several months. In section I, the LabJack UE9 and its functionality are discussed. The application of the instrument within our research group is presented along with a synopsis of the progress to date.

The LabJack UE9 is an electronic module that simplifies the measurement of voltages in the laboratory. Thus, in combination with an appropriate transducer, it can be used to measure temperature, pressure, or other quantities of interest. We presently use it to measure chamber pressures by converting analog output voltages from pressure sensors to digital information which is then stored on a computer. This conversion allows us to monitor the chamber pressure remotely, a feature that is important as the vacuum chamber is operated in a radiation field. This task was performed in preparation for an experiment at Lawrence Berkeley National Lab.

The second section of this report details the development and testing of an electronic device referred to as the "pulser head." This device, developed by the Nuclear Chemistry group, together with the Electronic Instrument Services in the Chemistry Dept., is intended to improve the efficiency of calibrating highly segmented Silicon arrays. The pulser head consists of solid-state relays in an electronic circuit that will allow remote switching between discrete electronic channels, minimizing the plugging and unplugging of cables on charge sensitive detectors and electronics.

I. LabJack Overview

The LabJack UE9 is a USB/Ethernet based measurement and automation device that affords a user-friendly interface between a computer and the physical world. It is used to read the output voltage of sensors that measure a wide range of physical quantities (e.g. temperature, pressure, etc.). It accomplishes this via several analog input lines. Any analog voltage on these inputs can be digitized. The resulting digital information is read out by the PC and can be both processed and stored. The LabJack UE9 can also be used to control lab instruments as it has several digital I/O lines along with analog outputs. We are principally interested in measuring the output voltage from a source (pressure transducer) to remotely monitor the pressure in a vacuum chamber.

Figure 1. LabJack UE9 [1].

The LabJack was chosen because of its simplicity of operation and its Linux compatibility. These features, along with its input voltage range, made it well suited to the intended tasks. The LabJack was intended to replace existing ISA ADC cards. ISA devices are quickly becoming obsolete due to the integration of faster and more efficient interfaces such as PCI and USB. Consequently, newer computers routinely do not have

ISA slots on their motherboard, creating an upward migration problem. The LabJack can perform the same ADC functions while bypassing the need for an ISA connection, thus helping our ADC requirements for future projects and experiments.

LabJack Specifications

The LabJack UE9 has three general input/output (I/O) sides: the communication side, the screw terminal side, and the DB side. On the communication side, there is a USB type B port, an Ethernet 10Base-T port, and two external power connectors, including a screw terminal and a power jack. The screw terminal side contains six blocks of screw terminals with four terminals per block. Included are four analog inputs, two analog outputs, and four digital I/O. And the DB side consists of two DB connectors: a DB37 and a DB15. The DB37 connector contains all of the analog I/O and some digital I/O, and the DB15 provides 12 digital I/O.

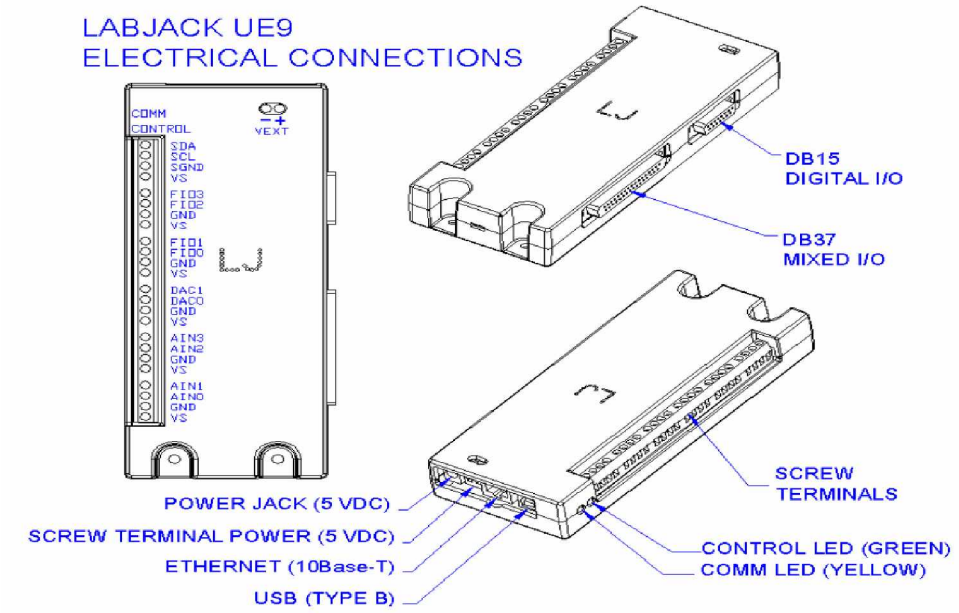

Figure 2. LabJack UE9 connections [1].

The USB port is compatible with both USB version 1.1 and 2.0, and it has the ability to provide both power and communication. When connected to a PC via USB, the UE9 will [generally] share ground with the PC and is thus not electrically isolated. The 10Base-T Ethernet connection provides only communication, so power must be supplied either through a USB cable or via an external power supply. In our setup, we installed a network interface card (NIC) on the PC and connected the LabJack directly to it via a crossover cable in order to have communication. For the power supply, there is a two-pole screw terminal and a center-positive power jack that are both electrically common. The nominally required power supply is +5 volts direct current (VDC) at 200 milliamperes (mA) or less, with a minimum measurable voltage of -0.01V and a maximum measurable voltage of 5.07V, not to exceed 5.50V.

Grounding information is as follows. All available GND connections on the UE9 are common with each other so, if the USB is providing power, the UE9 shares ground with the PC and, if there is an isolated power supply, the UE9 will not in general share ground with the PC. There are GND connectors at the screw terminals and in all the other ports mentioned.

There are 16 analog inputs, 14 of which are user-accessible at the DB37 connector. Four of these analog inputs can also be accessed via the screw terminals. Thus, the user should exercise caution when accessing the first four AIN (AIN0-AIN3), as these are electrically the same. The remaining two AIN (AIN14-AIN15) are connected internally. The UE9 contains 16-bit ADCs and converts analog input signals directly to binary values, so voltage conversion can be approximated as follows:

$$\text{Volts(uncalibrated)} = (\text{Bits} / 65536) * \text{Span} ,$$

where Span is the difference between the maximum voltage and the minimum voltage. However, to obtain more accurate voltage conversions, it is best to use the calibration constants (slope and offset) stored in the Mem area of the UE9 to calculate the voltage:

$$\text{Volts(calibrated)} = (\text{Slope} * \text{Bits}) + \text{Offset}$$

The AINx on the LabJack measure voltages with respect to UE9 ground, so signals can be accurately measured as long as the input voltage falls within the specified range. The resolution within this range can be shown in terms of voltage. Suppose we have a 0-1V input signal that is being acquired within the 0-5V input range at 16-bit resolution, then the voltage resolution can be shown as 5V/65535bits = 0.076mV/bit, which yields about 13,100 discrete steps over the 1V signal span.

Testing linearity of channels on the LabJack

In order to check that the LabJack UE9 voltage measurements are accurate, we tested the linearity of channels AIN0-AIN3 by supplying 0-5.5VDC with a high precision DC power supply, recording the ADC value at each voltage, and then plotting the voltage as a function of ADC value along with the relative percent error (RPE). The results for AIN3 are shown in Figure 3. The UE9 accepts a measurable voltage input range of 0-5.00V, and the ADC saturates at 5.10V and is linear from 0-5.09V for the aforementioned AINx channels.

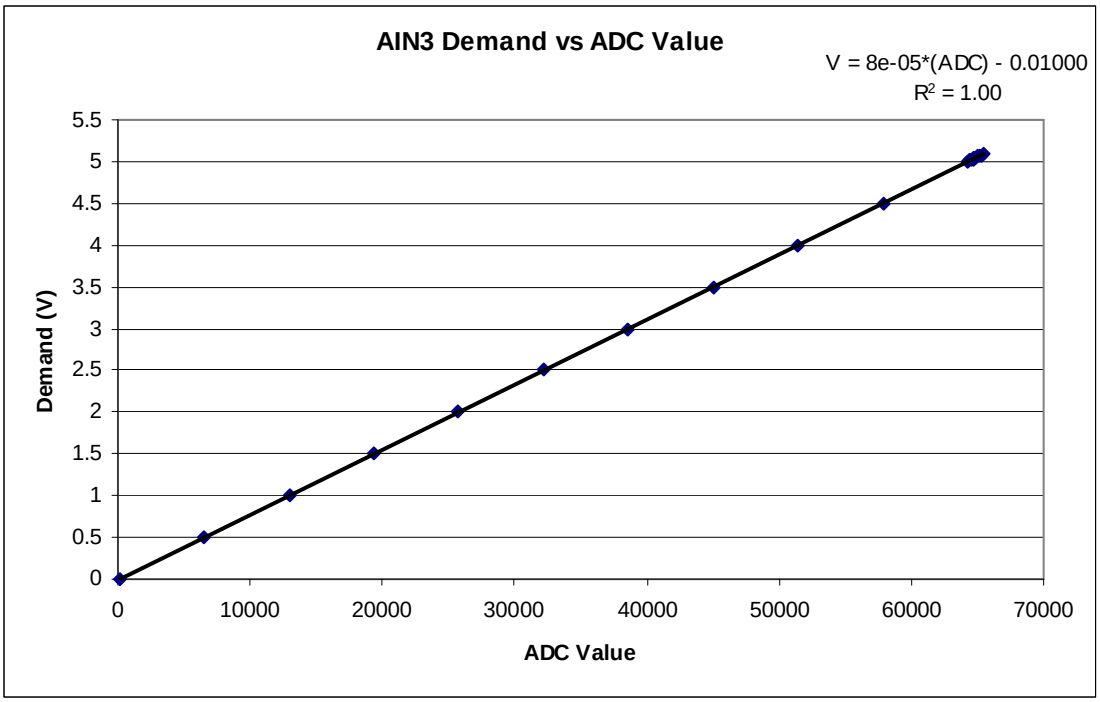

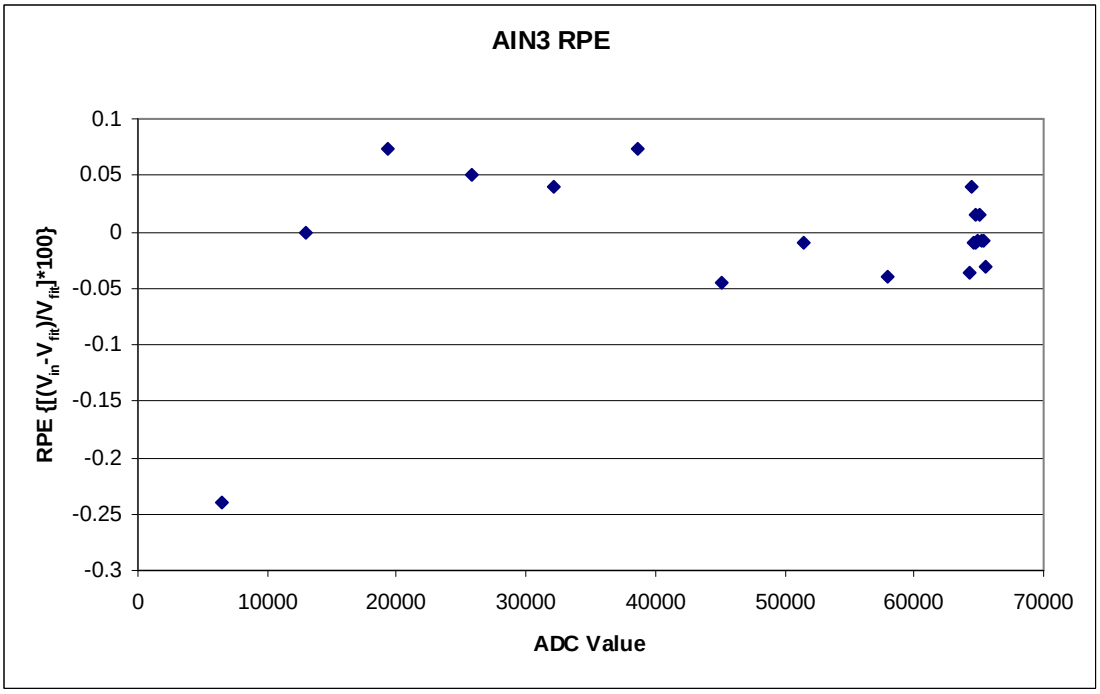

Figure 3. LabJack UE9 linearity test for AIN3.

LabJack at LBNL

Nuclear science experiments are typically carried out in scattering chambers evacuated to low pressures. Moreover, these chambers, when an experiment is being conducted, exist within a radiation field and are operated in a secured environment. Measurement of the chamber pressure therefore needs to be conducted remotely. To address this need, we placed a computer in the radiation area adjacent to the scattering chamber. The UE9 was interfaced to this computer with various pressure sensors connected to the UE9's inputs. This local computer was then networked with another computer in a radiation safe environment via Ethernet.

The LabJack was controlled by a computer program written in the C programming language and was interfaced to the local computer via a second NIC utilizing TCPIP. The UE9 was physically connected to the local computer via a cross-over cable. Power was supplied by the USB cable, and a graphical user interface to simplify control of the UE9 was written in the Tcl programming language. This code presently allows the user to monitor one analog input channel of the LabJack but can be expanded to monitor multiple channels.

The experimental setup involved connecting a maximum of four vacuum pressure gauges to the screw terminal analog inputs (AIN0-AIN3). The pressure gauges were three Series 917 Pirani vacuum sensors connected to different parts of the chamber system. Testing prior to the experiment was conducted using one such Pirani sensor in our laboratory at IUCF. To assess the accuracy of the voltage measurement by the LabJack, we used a precision DC power supply (Power Designs, Inc., Model 2020B, Output 0-20VDC, 0-2A).

The Series 917 Pirani Vacuum Sensor System [2] connects to a controller via a cable with a female octal socket at one end and a male DB15 connector at the other, and we used pins 11 and 12 of the male DB15 accessory port at the rear of the controller to access the analog output for our UE9 analog input.

The Pirani sensor system measures the pressure from 10^{-3} Torr to 10^{3} Torr and provides a proportional analog DC voltage in the range of 0.03 V to 3.25 V. This output voltage range is well suited to the 0-5V input voltage range of the UE9. The conversion between voltage and pressure was incorporated into the control program for the UE9, allowing direct display of the chamber pressure. In order to calculate the pressure, we used the factory calibration data points for N_2 gas and plotted the pressure as a function of voltage on a semi-logarithmic scale. Since fitting the calibration data was difficult due to the non-linearity at both small and large voltages, we elected to use an interpolation procedure to convert voltage to pressure. The measured voltage was compared to calibration data voltages and, if the voltage input fell between a particular pair of points, linear interpolation was used to calculate the corresponding pressure.

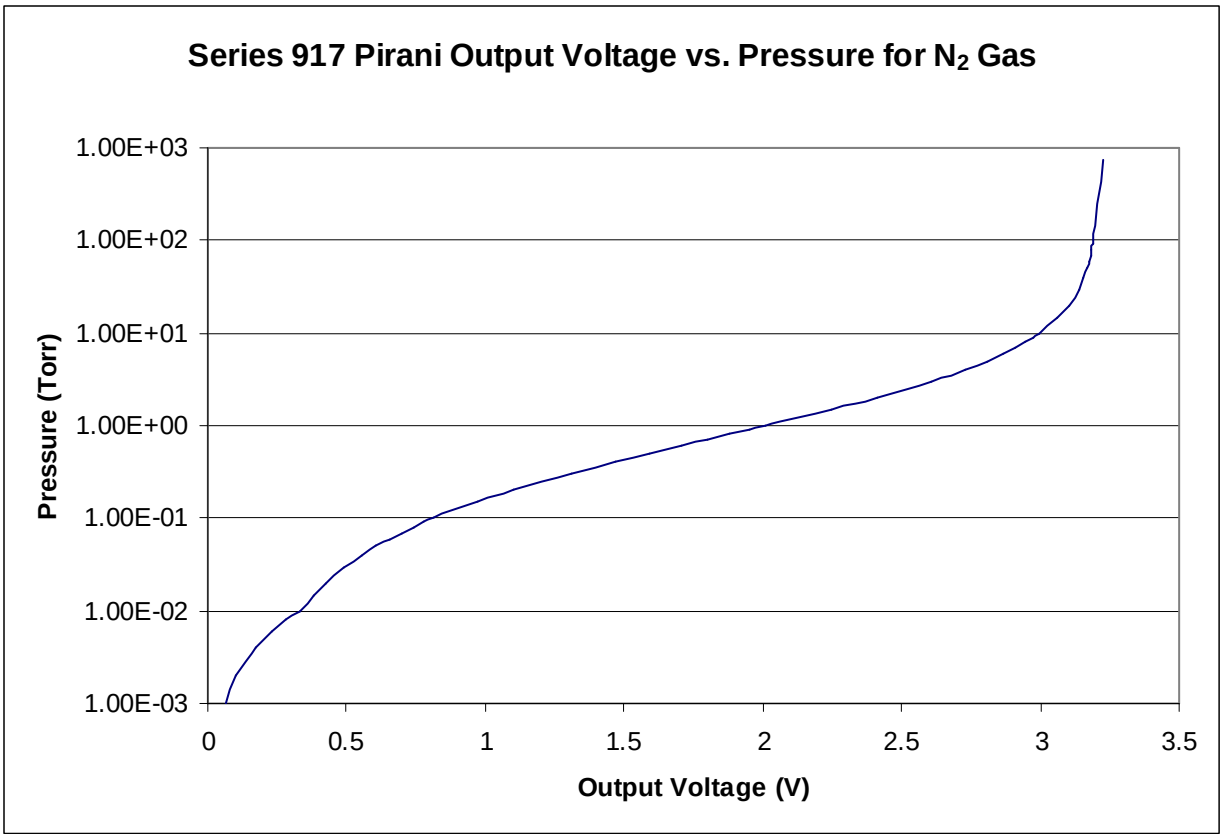

Figure 4. Plot of data used for voltage-to-pressure conversion [2].

Monitoring the Pirani sensors is effective if we encounter a chamber leak, which results in a pressure excursion $P>1x10^{-3}$ Torr. We generally run between 10^{-5} Torr to 10^{-6} Torr, so we would also like to monitor the chamber in this pressure range. If a leak occurs, a pump fails, or there is a vacuum excursion for any other reason, then we will be able to see it before some sensitive detectors or electronics are destroyed. Therefore, we also plan to implement monitoring of an ion gauge controller in an upcoming experiment because the ion gauge is sensitive to much lower pressures. So, we will need to modify the current control program to include a method to calculate the pressure in this range.

II. Pulser Head Overview

Developing a New Technique for the Charge Calibration of Highly Segmented Silicon Arrays

Segmented detectors are increasingly used in nuclear science to provide improved angular resolution. This improved angular resolution dramatically impacts the ability to measure short-lived quantum states through the use of particle-particle correlations. As detector segmentation increases the number of electronic channels also increases, leading to the difficulty of calibrating a large number of electronic channels. Over the past decade, segmentation has increased from <100 channels to >1000 channels. It has therefore become necessary to develop a more efficient method to calibrate the electronics associated with a highly segmented detector. The objective of this project is to calibrate a segmented Silicon detector using a prototype pulser head and compare the results to those obtained using conventional methods.

The conventional method of detector calibration involves the use of standard radioactive sources and/or sending a well-defined voltage from a precision charge pulser into a charge-sensitive amplifier (Fig. 5) and acquiring the resultant signal for one channel; a channel is accessed via a 2-pin connection from a 34-pin connector. By increasing the applied voltage (increasing the pulse amplitude) in a controlled fashion, we can calibrate that one channel by determining the linearity of the response. The absolute reference is provided by the well known decay energy from an alpha source. This task must then be repeated for each channel in the system. Also, as it is necessary to manually disconnect and reconnect each channel at its input, the possibility exists of inverting the ground and signal pins, thus discharging the detector. Unbiasing the detector in this manner is not only an expenditure of time but could damage either the detector or the electronics. Thus, it has become time-prohibitive to calibrate detectors of several hundred channels or more using conventional techniques. Both the FIRST (Forward Indiana Ring Silicon Telescope) array [3] and LASSA (large area silicon strip array) [4] represent new detector arrays constructed by the Indiana group that require a new approach to calibration.

To overcome this inefficiency, a pulser head/charge terminator prototype has been designed and constructed by the IU Chemistry Electronic Instrument Services shop in conjunction with the Nuclear Chemistry group. This pulser head consists of eight solid state relays, each connected to an individual electronic channel. These relays allow the user to remotely switch from one channel to the next in order to calibrate all of the electronic channels without physically manipulating the connections after a single channel is calibrated. We have also improved our past calibration technique by improving the pulser connected to the pulser head. The two notable changes to the pulser are an increase in its frequency from 100Hz to 500Hz and an improvement in the signal-to-noise ratio (S/N) by a factor of approximately 3. Using this new approach, we estimate that a calibration that would have taken conventionally about 9 man-days using the conventional approach will now be reduced to about 8 man-hours, a substantial reduction in time expenditure. Moreover, the risk of an improper manual connection is greatly reduced. Although the pulser head will reduce the amount of time spent calibrating the detector, there still exists the likelihood that it will be a source of electronic noise that may reduce the resolution of measurements with respect to a data acquisition arrangement without its presence. Thus, the present goal of the project is to compare the calibration of a Si detector performed using the conventional approach and using the modified technique with the pulser head. Incrementally varying the amplitude of the pulse at each channel will allow the determination of the linearity and the gain and, by performing this for both calibration techniques, the possible resolution degradation and increased background noise from the pulser head can be determined.

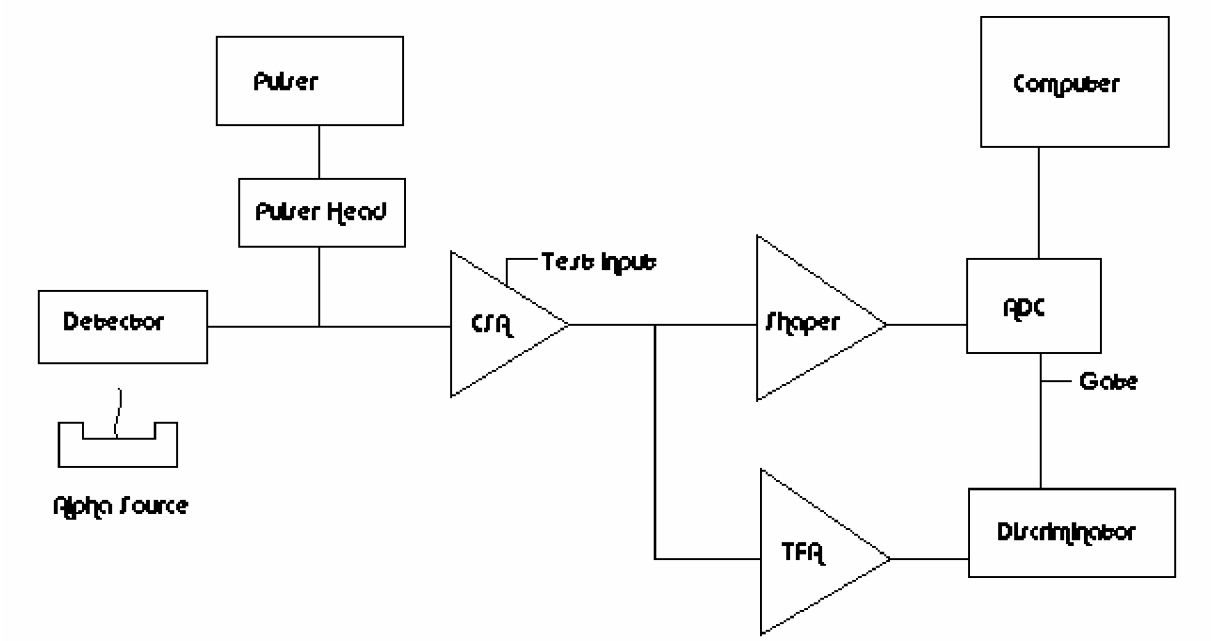

Figure 5. Schematic of the signal processing pathway, including the charge-sensitive amplifier (CSA), the shaping amplifier, the timing filter amplifier (TFA), and the analog-to-digital converter (ADC).

Should improved calibration efficiency, reduction in time, and minimization of background noise be achieved as hoped with the pulser head, this new technique will then be employed to calibrate the FIRST [3] array for upcoming research.

Pulser Head Testing Setup

The pulser head consists of a prototype board onto which an electronic circuit has been wired. The circuit consists of 8 solid-state relays for 8 signal channels and, as these relays open and close, they effectively switch from channel to channel (see Fig. 6). This board is encased in an aluminum box, from which the user has access to a step input, a pulse input, a male 34-pin connector, and +5V/GND inputs. The step input receives a pulsed signal from the pulser that causes the pulser head to switch sequentially from channel to channel, and there are 4 LEDs visible through the box that display in binary the

live channel (0-15) number. On the 34-pin connector, only even channels 0-14 are live due to the fact that the relays are physically too large to fit 16 side-by-side to access all 16 channels. The pulser head also has its own charge terminator to convert the input voltage pulse from the pulser into a charge pulse prior to the charge-sensitive amplifier (CSA) input. If the present tests are successful, we intend to alter the geometry of the pulser head to accommodate 16 channels. The testing setup is presented in Fig. 7. There are three pulsers that were used: a stability pulser, a calibration pulser, and an Ortec research pulser. The stability pulser was built at IU for the Nuclear Chemistry group, offers the poorest resolution of the three, and is capable of a maximum frequency of 100Hz. The Calibration pulser also was custom-built at IU but offers better resolution by a factor of three and is capable of a maximum frequency of 500Hz. We intend to use this pulser with the pulser head in upcoming experiments. The Ortec pulser is a high-quality commercial research pulser that will be used as a reference point for the other two pulsers. Operation of the Ortec pulser is completely manual, and it has a maximum frequency of 100Hz.

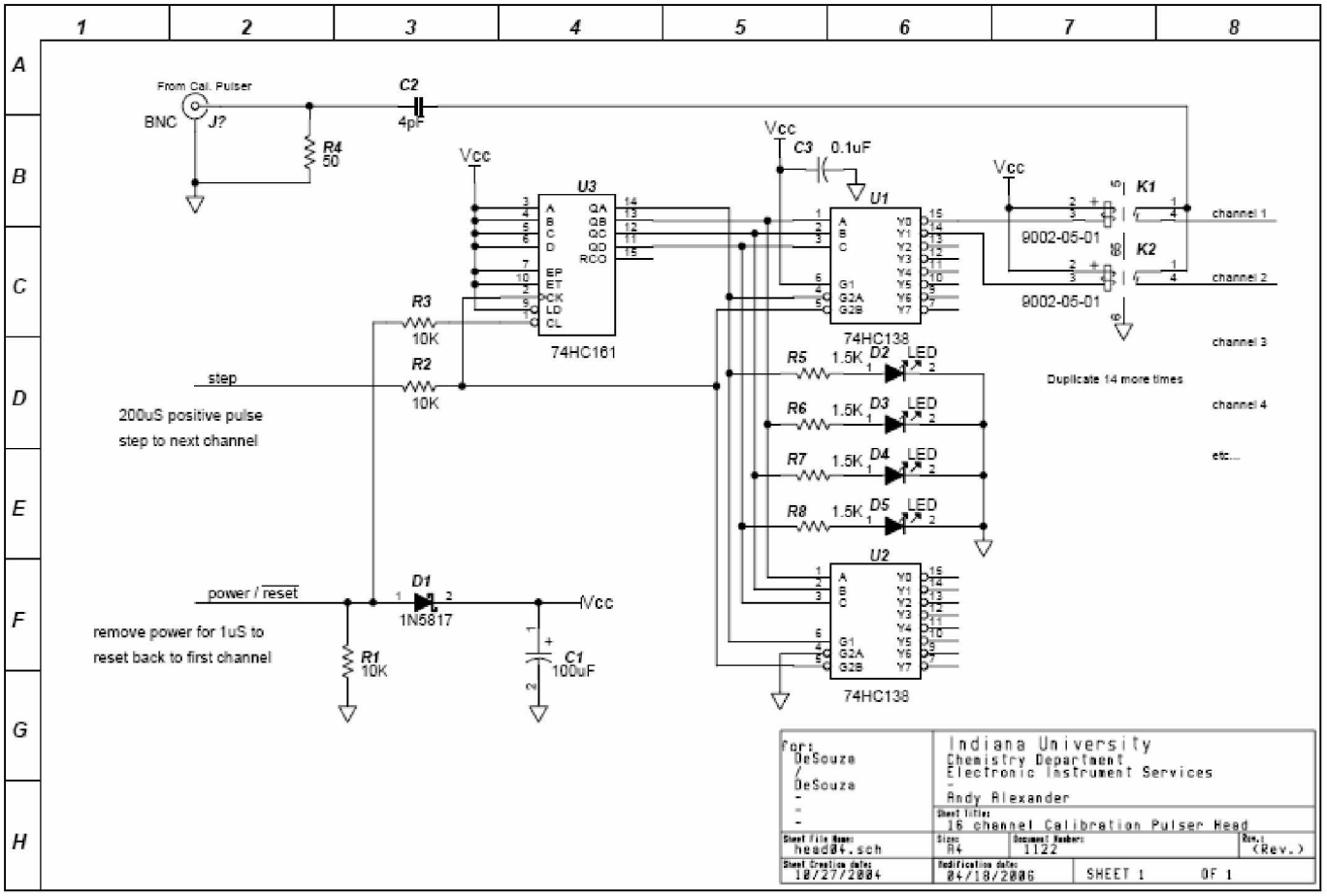

Figure 6. Pulser Head schematic.

The first task was to check the signal on every channel and make sure that there was no electronic cross-talk between adjacent channels. All the active channels showed almost identical signals with 31.6mV amplitudes and about 200µs rise times. This particular testing setup starts with the IU stability pulser and can be seen in Fig. 7. The step signal comes from the Pulser Sync Out port and, because it is a NIM-type logical signal and the pulser head requires a TTL signal, a level translator had to be used to convert from one logic family to the other. A down scaler was used to control the number

of pulses before the pulser head would change to a different channel. The down scaler was typically set to about 80-100, resulting in the channel being switched at about 1Hz. The analog pulser output was connected to the PULSE input of the pulser head, and a +5VDC power supply was used to power the pulser head. The pulser head is placed inside of a vacuum chamber, with its input signals provided via a BNC flange. Then, a ribbon cable runs from the 34-pin connector on the pulser head connected to the true input of the CSA via a short 34 conductor ribbon cable. Powered by ±12V, the CSA is inverting, resulting in a negative signal at the output of the CSA. This signal is processed by the electronic chain shown in Fig. 5. All of the channels were tested for noise and cross-talk by viewing the signals from the CSA output on an oscilloscope, and channels 8 and 14 were randomly selected to test the linearity of their response. The following plots in Fig. 8 illustrate the pulser input voltage as a function of the DAC setting (pulse amplitude), the input voltage as a function of the CSA voltage, and the RPEs as a function of the DAC setting.

The next step in testing was to connect the pulser head to a Silicon detector in the evacuated vacuum chamber, place the detector in front of a standard radioactive alpha source (^{241}Am), and obtain the signals through the entire electronics chain as in Fig. 5.

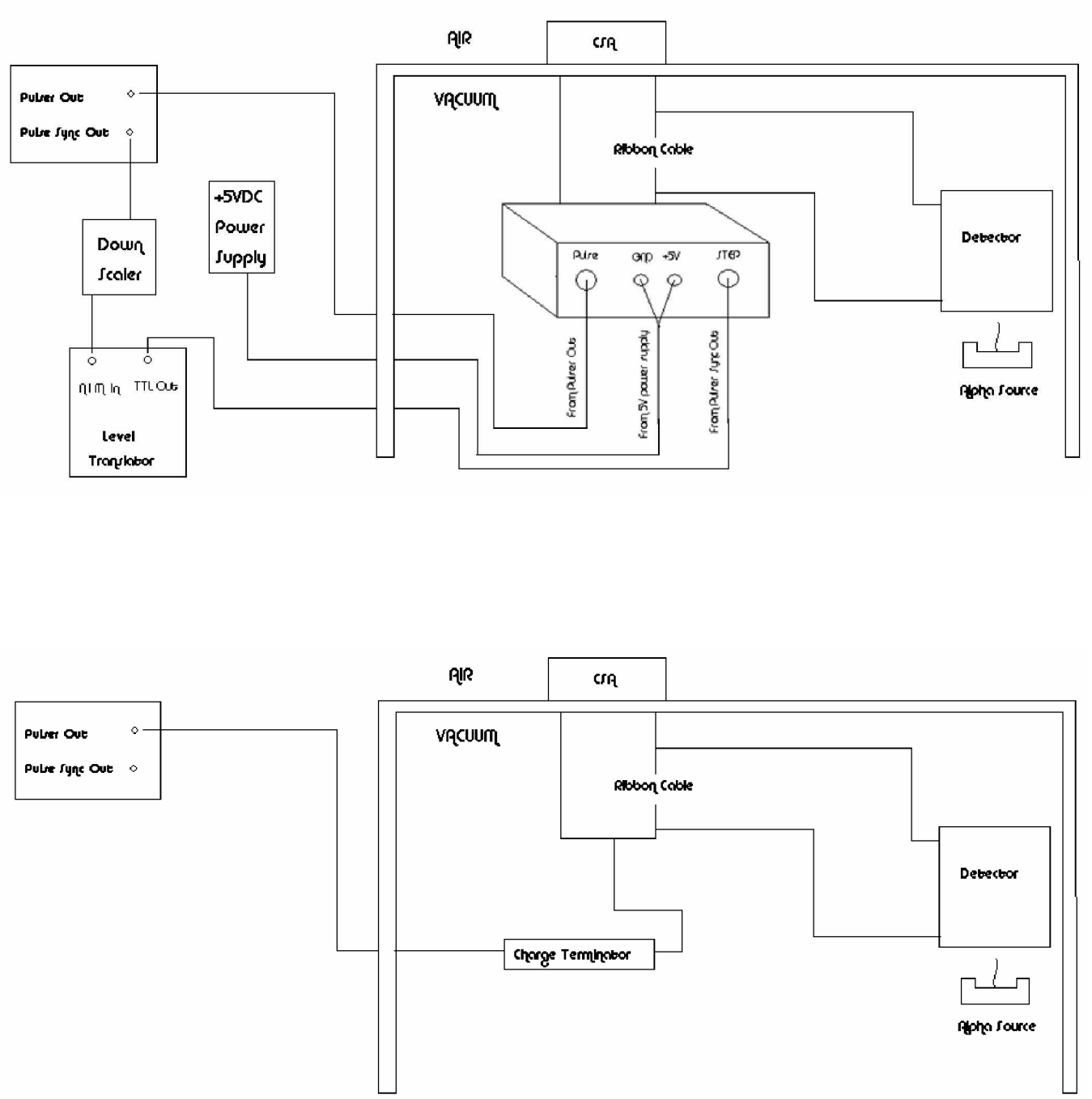

Figure 7. Signal path just forward of CSA in Fig. 5. Top: Testing setup with detector and pulser head/charge terminator in place. Bottom: Testing setup with detector and charge terminator in place.

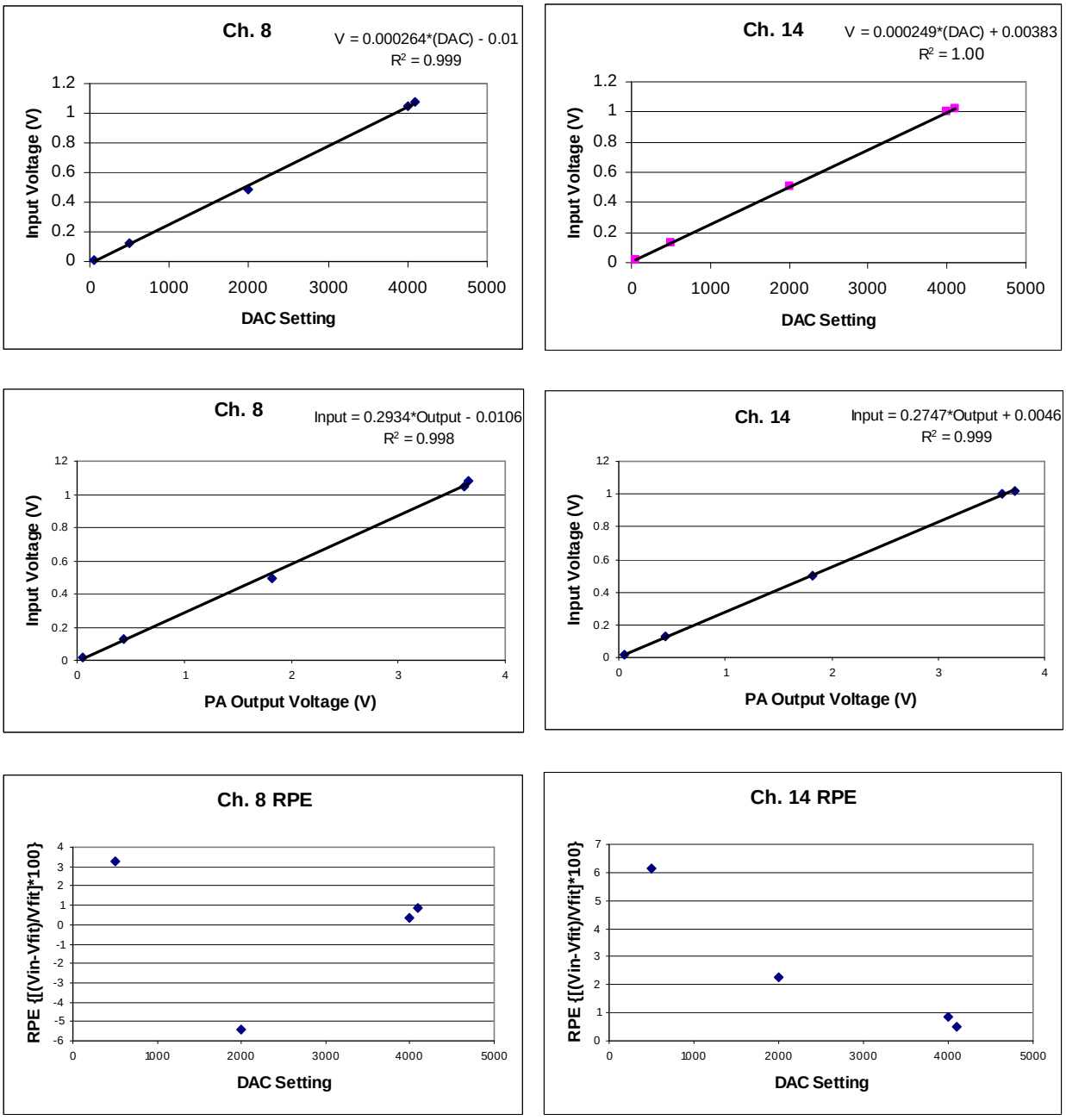

Figure 8. Pulser head input voltage vs. DAC setting, input voltage vs. CSA output voltage, and RPEs for channels 8 and 14.

Silicon Detector

The Silicon detector used is a double-sided LASSA detector 500 microns thick

[4]. It is basically a Silicon diode and, when unbiased, exhibits a ~0.6V junction potential.

The alpha particles were first observed on the oscilloscope from the CSA output and, as expected, were negative in polarity. The detector responds to the holes generated from the electron-hole pairs created when the alpha particle ionizes the matter of the detector as it loses its kinetic energy. So, there is a positive input voltage that gets inverted through the CSA. Because the detector is unbiased, most of the electron-hole pairs immediately recombine, and only a few events are seen on the oscilloscope. The signals that are observed are small in amplitude, on the order of millivolts. There is also quite a bit of electronic "white noise" (pp ~75mV) due to the CSA and detector capacitance. Thermal electrons having sufficient energy surpass the junction potential and are the main source of this "white noise." In order to decrease the noise and increase the signal amplitude, the Silicon detector must be reverse-biased (Fig. 9) by applying a negative voltage with respect to the p-side of the diode (as in diagram B of Fig. 9). This effectively increases the junction potential and cuts down on thermal electronic noise and, more importantly, stops most recombination by sweeping the negative and positive charges in opposite directions due to the applied electric field. Depending on the magnitude of the supplied detector bias, different alpha signal amplitudes will be seen. The higher the detector bias, in general the higher the signal amplitude (i.e. less recombination). However, when the detector bias is sufficient to eliminate recombination, applying yet more bias will not increase the signal amplitude further. When the detector has zero bias, as stated above, the junction potential is ~0.6V, and there exists a region over which there are very few holes and electrons due to the electric field that is created.

This region is the depletion region (the area in white in Fig. 9), and it will grow larger as the negative bias to the diode is increased, with simultaneous attenuation of

recombination. The diode can be sufficiently reverse-biased to the point that the entire volume of the detector is a depletion region. However, this is unnecessary because the point at which zero recombination is reached is not necessarily the point at which the entire detector is a depletion region. The alpha particles have a definite kinetic energy and thus only penetrate into the detector through a certain thickness. Therefore, a much lower detector bias is sufficient to provide a sufficiently deep depletion region and effectively reach zero recombination. This is important because when dealing with high voltages under vacuum, there is a potential to spark. This easily can damage the detector(s) and other electronic components, so it is best to minimize the applied voltages when possible.

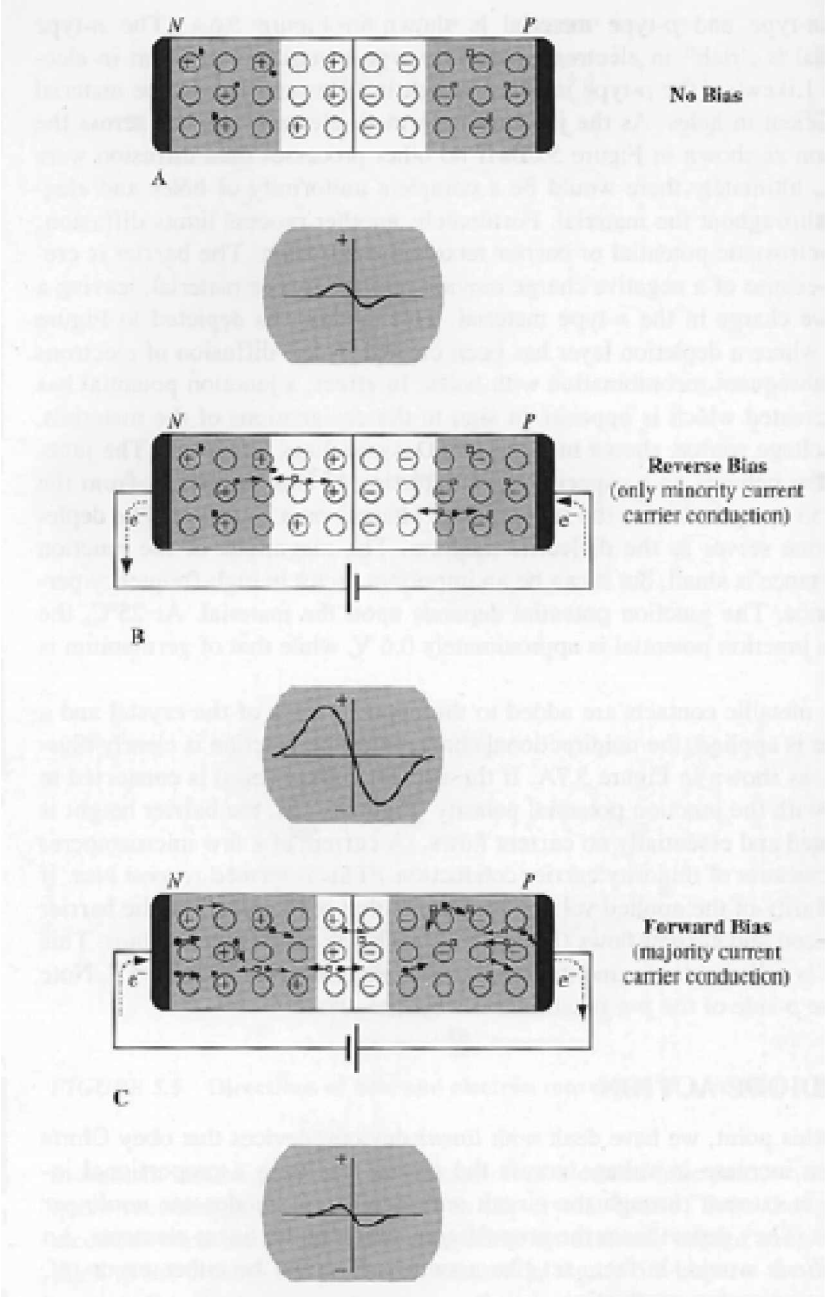

Figure 9. The p-n junction potential under differing applied voltages [5].

Results

Several spectra were taken using the three different pulsers, a standard radioactive source, and with the pulser head present and then not present in the signal processing

pathway. The pulser head's contribution to the electronic noise could be determined by taking the difference between the resolution obtained from the pulser head present in the signal chain and the resolution obtained from the charge terminator in its place. In the first series of tests, the pulser head was connected to the detector, which was placed in front of an ^{241}Am alpha-emitting source inside of the vacuum chamber. After evacuating the chamber to $<10^{-4}$ Torr and negatively biasing the detector to -45V, the alpha signals were seen on the oscilloscope. To closely approximate the alpha signal amplitude, the pulser amplitude was set so that its signal amplitude was slightly less than the alpha signal amplitude. This ensures that the ADC channels used during data acquisition for the both the pulser signal and the alpha signal are relatively close so that calibration using the pulser is certain to be accurate within this range. Similarly, these same measurements were taken with the charge terminator in place of the pulser head (again, accounting for the proper amplitude setting on the pulsers to match the signal amplitude of the alphas). Table 1 below lists the pulser conditions. To find the percent resolution, the following formula was used:

$$\%\text{Resolution} = (\text{FWHM} \div \text{Centroid}) * 100$$

The energy resolution in keV was also determined using the following:

$$\text{Resolution (keV)} = (5.4\text{x}10^{3}\ \text{keV} \div \text{Centroid}) * \text{FWHM} \quad ,$$

where the alpha decay energy of ^{241}Am is known to be 5.4MeV, and the assumption is made that 0MeV corresponds to ADC channel 0. Typically, the zero-point is determined using two or more standard sources. In Table 2 below, the results using the pulser/pulser head setup and the pulser/charge terminator setup are shown. During our testing, it was observed that the computer monitor was a major contributor to the noise in the system.

The pulser head measurements were obtained with the shaper/discriminator control computer monitor on and, due to time constraints, these measurements were not reproduced with the monitor off. However, to qualitatively show the effect of the noise introduction with this monitor being on, the charge terminator measurements were repeated with the monitor on and off.

Pulser Head Conditions	**DAC Setting**	**Attenuation**	**Frequency (Hz)**
Stability Pulser	1800	x10	100
Calibration Pulser	640	x10	500
Ortec Pulser	1250	x10 x1.4	100
Charge Terminator Conditions			
Stability Pulser	2300	x10	100
Calibration Pulser	810	x10	500
Ortec Pulser	1250	x10 x1.2	100

Table 1. Pulser conditions for testing.

Measurements with Pulser Head	**FWHM**	**Centroid**	**Resolution (%)**	**Energy Resolution (keV)**
Stability Pulser, Monitor On				
α = alpha particle	16.68	2973.63	**0.561**	**30**
pulser	9.74	2414.74	**0.403**	**22**
Calibration Pulser, Monitor On				
α	17.48	2975.96	**0.587**	**32**
pulser	9.47	2626.91	**0.360**	**19**
Ortec Pulser, Monitor On				
α	n/a	n/a	n/a	n/a
pulser	**11.97**	**2526.07**	**.474**	**26**
Measurements with Charge Terminator				
Stability Pulser				
Monitor On				
α	18.65	2913.90	**0.640**	**35**
pulser	12.45	2466.02	**0.505**	**27**
Monitor Off				
α	n/a	n/a	n/a	n/a

	pulser	n/a	n/a	n/a	n/a
Calibration Pulser					
	Monitor On				
	α	21.80	2912.01	**0.749**	**40**
	pulser	14.97	2658.13	**0.563**	**30**
	Monitor Off				
	α	25.59	2909.43	**0.880**	**47**
	pulser	9.87	2656.85	**0.371**	**20**
Ortec Pulser					
	Monitor On				
	α	39.60	2908.94	**1.361**	**74**
	pulser	11.10	2644.31	**0.420**	**23**
	Monitor Off				
	α	26.25	2910.63	**0.902**	**49**
	pulser	8.56	2643.63	**0.324**	**17**

Table 2. Results of spectra taken with three pulsers for the pulser head and charge terminator.

As can be seen from the data table in Table 2, the alpha peak location (centroid) remains relatively constant, differing mainly due to the inconsistency in the cuts that we made when integrating the peak areas. Had the alpha peaks shifted, then some electronic drift would be suspect. The alpha resolution is poorer than the pulser resolution, as is also expected, due mainly to detector capacitance. It appears that the measurements made with the charge terminator are actually poorer in resolution than those made with the pulser head in-line. Furthermore, the three pulsers show worse resolution with the charge terminator measurements than with the pulser head measurements. However, when the charge terminator was put into place in the vacuum vessel, a longer LEMO cable was needed when making the BNC→LEMO→2-pin connection at the charge terminator output to the ribbon cable input of the CSA, and this would likely result in such an introduction of excess noise. In subsequent testing, this issue will be addressed.

Introduction of the pulser head into the signal chain arguably contributes insignificantly to the inherent electronic noise and, thus, will most likely be modified to better suit our research needs and then retested in a similar fashion. Shown in Figs. 12 and 13 below are the spectra obtained from the testing setup as described above. The left-most peak in all the spectra corresponds to the pulser signal, and the right-most peak corresponds to the alpha signal. The noticeable double peak (and third shoulder peak, if resolved) of the alpha spectrum is due to the differing alpha decay energies—85% at 5.48MeV, 13% at 5.44MeV, and 1.6% at 5.39MeV. Also, the marked difference between resolution with the monitor on and with the monitor off can be seen in Fig. 13.

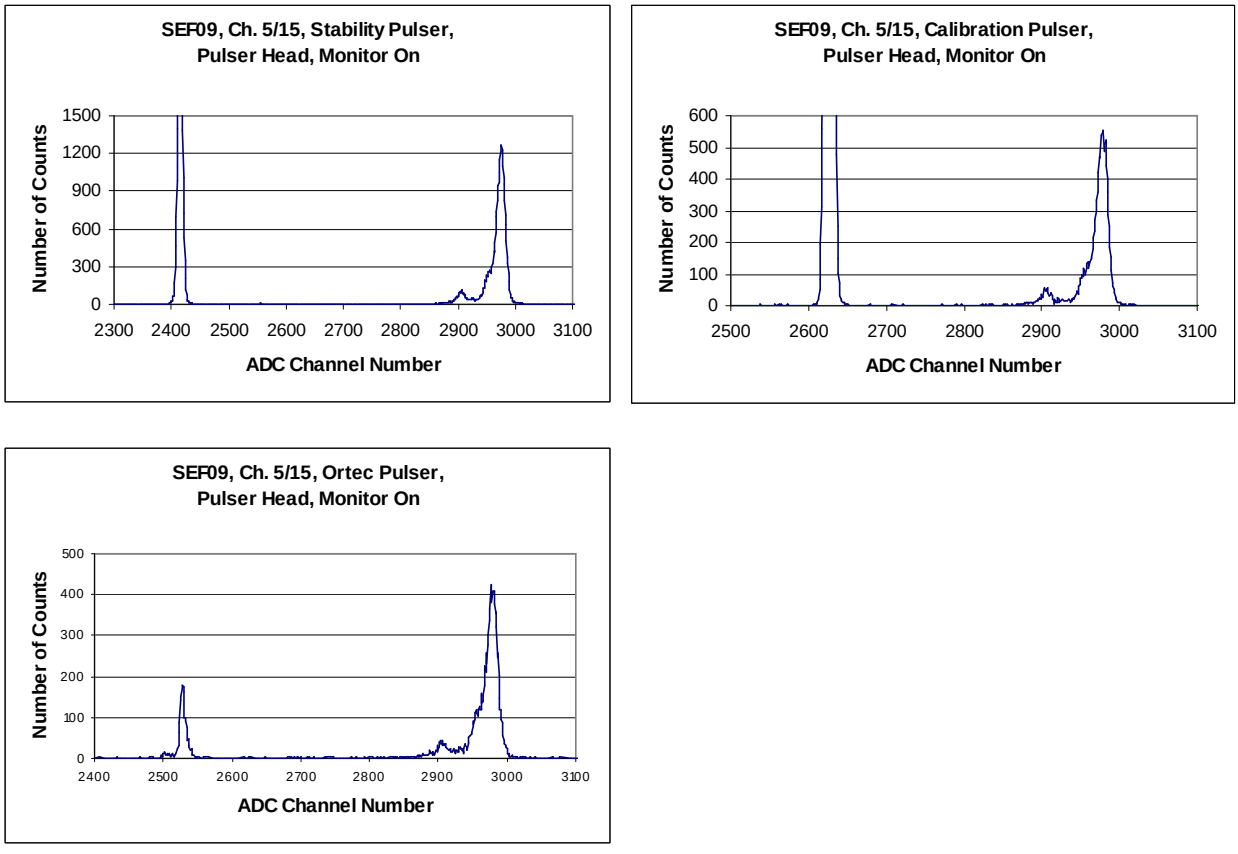

Figure 12. Spectra for pulser head measurements with the monitor on.

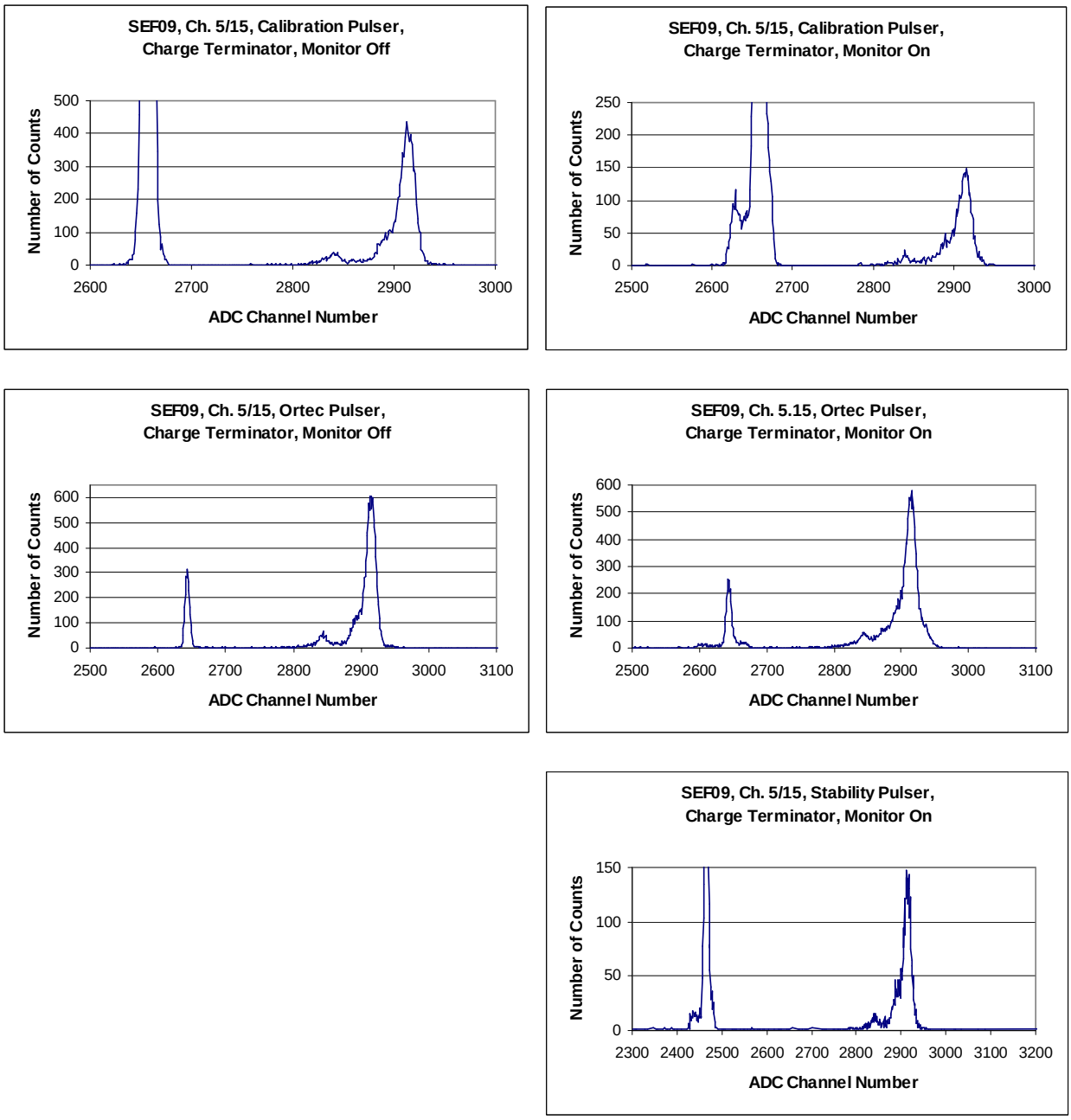

Figure 13. Spectra for charge terminator measurements with both the monitor on and with the monitor off.

Conclusions

The LabJack control program is in working order, but the Tcl code has yet to be sufficiently modified. It currently works with one channel but will need to be expanded to

work with several channels. Additionally, our current hardware allows us to measure at most four sensors by connecting them directly to the four screw terminal AINx channels. The DB37 connector contains all 14 user-accessible AINx so, ideally, we could measure 14 different pressure sensors (or the output voltages of other sensors, as well) if the hardware can be adapted correctly.

Initial results from testing the pulser head also look promising. It does not appear to be a significant contributor to electronic noise, but further testing needs to be performed in order to confirm this conclusion. Additionally, because this is a prototype, it will need to be modified in order to take advantage of using the maximum number of channels possible on one board. The input connections may also be modified so that there exists enough space to use the appropriate connectors. These issues will be addressed in the coming months.

References

[1] http://www.labjack.com/labjack_ue9.html, Copyright 2001-4, LabJack Corporation.
[2] http://www.mksinstruments.com/pdf/917.pdf.
[3] B. Davin, R.T. de Souza, R. Yanez, y. Larochelle, R. Alfaro, H.S. Xu, A. Alexander, K. Bastin, L. Beaulieu, J. Dorsett, G. Fleener, L. Gelovani, T. Lefort. J. Poehlman, R.J. Charity, L.G. Sobotka, J. Elson, A. Wagner, T.X. Liu, X.D. Liu, W.G. Lynch, L. Morris, R. Shomin, W.P. Tan, M.B. Tsang, G. Verde, J. Yurkon, Nuclear Instruments and Methods in Physics Research A 473 (2001) 302.
[4] T. Paduszynski, P. Sprunger, R.T. de Souza, S. Hudan, A. Alexander, B. Davin, G. Fleener, A. Mcintosh, C. Metelko, R. Moore, N. Peters, J. Poehlman, J. Gauthier, F. Grenier, R. Roy, D. Thériault, E. Bell, J. Garey, J. Iglio, A.L. Keksis, S. Parketon, C. Richers, D.V. Shetty, S.N. Soisson, G.A. Soulioutis, B. Stein and S.J. Yennello, Nuclear Instruments and Methods in Physics Research A 547 (2005) 464.
[5] Indiana University Nuclear Chemistry course notes (CHEM-C460), Lecture 7, Semester I, 2005, Professor Romualdo T. de Souza.